THERMODYNAMIC ANALYSIS OF A HYBRID PHOTOVOLTAIC/THERMAL SOLAR COLLECTOR

Luigi Marletta[1], Gianpiero Evola[1]

[1]Department of Industrial Engineering, University of Catania
Viale A. Doria, 6 – 95125 Catania (Italy)
*e-mail: gevola@unict.it

ABSTRACT

Hybrid photovoltaic/thermal collectors (PV/T) usually consist of common photovoltaic modules cooled by a suitable fluid, and convert solar radiation simultaneously into both thermal and electric energy. The heat transfer between PV cells and cooling fluid allows lowering the temperature of the PV cells, thus improving their efficiency; it also generates low-grade heat made available for specific applications. As a consequence, PV/T modules have a very interesting overall energy efficiency.

In this paper, the Second Law analysis of a water-cooled PV/T module is discussed; the study aims to underline one main drawback for the optimal exploitation of such a technology: the electricity production from PV cells increases at low temperatures, whereas the usability of the thermal energy is higher at high temperatures.

The results may allow a real optimization of PV/T collectors, and lead to the definition of those operational conditions that maximize the total exergy harvested by the system.

KEYWORDS

PV panels, mathematical modeling, heat recovery, exergy efficiency

1. INTRODUCTION

Hybrid photovoltaic/thermal collectors (PV/T) are devices that convert solar radiation simultaneously into thermal and electric energy. Basically, they consist of a thin plate made of highly conductive material, on top of which the PV cells are inserted by lamination; a series of channels is then welded on the other side of the plate, thus allowing the circulation of a fluid for heat removal. Such a fluid (usually air or water), while removing the excess heat from the PV cells, lowers their temperature and potentially improves their electric efficiency. In the same time, low-grade heat can be made available for appropriate uses. Figure 1 reports a simplified scheme of a water-cooled glazed PV/T [1].

When evaluating the performance of a PV/T collector, the definition of the coolant temperature is a main issue. Indeed, if one aims at producing hot water ready for technical applications, it should be necessary to operate at least around 40-50°C; however, such a temperature might penalize the electric performance of the PV cells. On the contrary, lower temperatures would allow better electric efficiency, but they would also affect the usefulness of the recovered heat.

In any case, the use of the PV/T technology allows to maximize the overall system efficiency, for a *given surface occupied by the collectors*, if compared to the separate production of electric and thermal energy by means of common PV and thermal collectors, respectively.

In the following, a discussion is presented concerning the thermodynamic analysis of a PV/T solar collector that is being developed in the framework of a national research program in Italy. In particular, the evaluation of the collector performance will be also based on the Second Law of Thermodynamics, as this approach can provide very interesting information about the optimal use of the system.

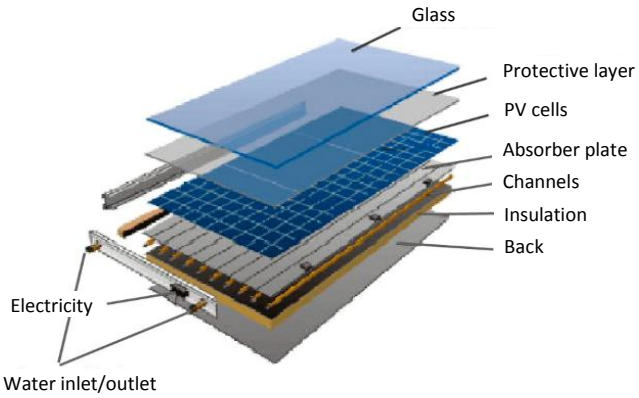

Fig. 1 – Simplified scheme of a water-cooled glazed PV/T collector [1]

2. THERMAL ANALYSIS OF THE PV/T COLLECTOR

2.1 *Description of the prototype*

In the framework of a national research project on "New Photovoltaic Technologies for Intelligent Systems Integrated in Buildings", a prototype of a water-cooled hybrid PV/T collector has been developed, designated for being integrated on concrete roofing systems in industrial premises.

Figure 2 reports a simplified scheme of the above-mentioned PV/T prototype. The coolant flows through a series of square channels made of stainless steel, with a thickness δ_c = 1 mm and whose outer side measures a = 10 mm. The channels are placed on a polystyrene panel appropriately shaped, while on their upper side they are pressed against a thin steel board (δ_p = 0.6 mm), that works as an absorber plate.

On the absorber plate a white painting is firstly applied (thermal emissivity $\varepsilon_p = 0.9$), then standard polycrystalline PV cells are laminated (156 × 156 mm). Finally, a 3-mm glazing is applied in order to cover and protect the absorber plate.

In Fig. 2 it is also possible to observe that the hydraulic connections for the fluid inlet and outlet are placed on the same side of the PV/T collector. As a consequence, six parallel paths are available for the circulation of the coolant, each one being twice as long as the length of the collector (L = 2966 mm, H = 1237 mm). In Fig. 3 the section of the left-hand half of the collector is shown, where the six square channels can be easily identified.

Furthermore, it is worth mentioning that not all the upper surface of the absorber plate is covered with PV cells. Thus, it is possible to define a parameter called Packing Factor (PF), that is the ratio of the total surface of the PV cells to the overall absorber surface. Since the collectors contains n_{PV} = 108 cells, the PF is:

$$PF = \frac{A_{PV}}{A_{tot}} = \frac{n_{PV} \cdot L_{PV}^2}{H \cdot L} = \frac{108 \cdot (156 \cdot 156)}{1237 \cdot 2966} = 0.716 \qquad (1)$$

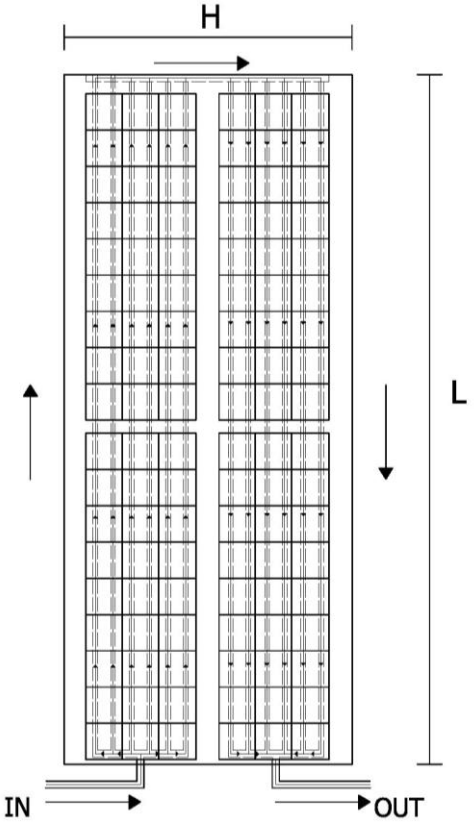

Fig. 2 – Simplified scheme of the PV/T prototype.

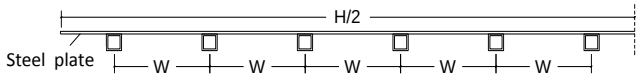

Fig. 3 – Simplified section of the PV/T prototype.

2.2 *Description of the mathematical model*

The mathematical modeling of the energy performance of the PV/T collector, aimed at the evaluation of the expected production of thermal and electric energy, needs the introduction of appropriate simplifying assumptions.

Firstly, let us assume that the absorber plate has a uniform space temperature distribution; this means that the surface temperature is unique for the whole PV/T, and this temperature can be attributed both to the absorber plate and to the PV cells applied on it.

Furthermore, the study of the thermal behaviour will be carried out on a control volume containing just one channel; however, the results can be easily extended to the other channels, thanks to the parallel hydraulic configuration. According to this hypotheses, Fig. 4 shows a simplified sketch of the control volume used for the mathematical modeling of the PV/T collector: it is composed of one square channel, whose length is 2 × L, together with a portion of the absorber plate having a width W = 79 mm.

Now, such a control volume is shaped as a fin, and the mathematical model for describing its thermal behaviour is known and discussed in [2] and [3]. In the following, the main equations are reported to describe the performance of the photovoltaic section.

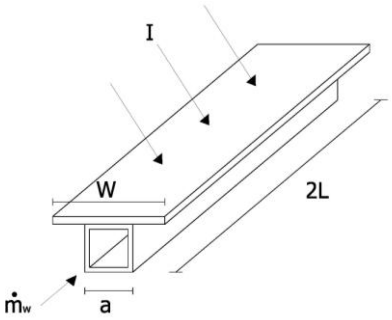

Fig. 4 – Control volume for the modeling of the absorber plate

First of all, with reference to Fig. 4, Equation (2) states the energy balance for the control volume in the time domain. In the left-hand side one can recognize the thermal power absorbed by the steel plate Q_{sol}, the heat losses to the outdoor environment Q_l, and the useful thermal power Q_w transferred to the water circulating inside the channel, detailed respectively in equations (3), (4) and (5).

$$\dot{Q}_{sol} - \dot{Q}_d - \dot{Q}_w = M_p \cdot c_{p,p} \cdot \frac{dT_p}{dt} \qquad (2)$$

$$\dot{Q}_{sol} = \underbrace{2L \cdot \left[(W - a) \cdot F + a \right]}_{\text{effective area}} \cdot I_{sol} \cdot \left[(\tau\alpha) - \tau_v \cdot \eta_{PV} \right] \qquad (3)$$

$$\dot{Q}_d = U_L \cdot (2L \cdot W) \cdot (T_p - T_a) \; \dot{Q} \qquad (4)$$

$$\dot{Q}_w = \dot{m}_w \cdot c_{p,w} \cdot (T_{out} - T_{in}) \qquad (5)$$

In Equation (3), due attention is paid to an important drawback related to the PV cells: since they convert a fraction of the incident solar radiation directly into electricity, they also determine a reduction in the thermal absorption capacity of the absorber plate. Such a reduction is obviously proportional to the electric efficiency η_{PV} of the PV cells, as reported in [4]. The latter depends linearly on the temperature T_p of the cells, according to the well-known relationship reported in Eq. (6): here, η_{STC} is the electric efficiency measured in standard conditions, and β is the temperature coefficient.

$$\eta_{PV} = \eta_{STC} \cdot \left[1 - \beta \cdot \left(T_p - T_a\right)\right] \quad (6)$$

Equation (3) also contains the so-called *fin efficiency F*, that accounts for the heat distribution along the portion of absorber shown in Fig. 4. The value of *F* is determined as a function of both the geometry and the thermophysical properties of the absorber plate (see Eq. 7).

In particular, U_L is the overall heat transfer coefficient of the collector, that can be calculated by means of Eq. (8) to (10). It is also necessary to assess the convective heat transfer coefficient $h_{c,g}$ on the outer surface of the collector, which depends on the wind velocity *w* [3] according to Eq. (11).

$$F = \frac{\tanh\left(m \cdot \frac{W-a}{2}\right)}{m \cdot \frac{W-a}{2}} \quad \text{con:} \quad m = \sqrt{\frac{U_L}{\lambda_p \cdot \delta_p}} \quad (7)$$

$$U_L \approx U_f \cdot \left[1 - (\psi - 45) \cdot \left(0.00259 - 0.00144 \cdot \varepsilon_p\right)\right] \quad (8)$$

$$U_f = \frac{1}{\frac{1}{h_{c,g}} + \frac{T_p}{344}\left(\frac{T_p - T_a}{f}\right)^{-0.31}} + \frac{\sigma \cdot \left(T_p + T_a\right)\left(T_p^2 + T_a^2\right)}{\frac{1}{\varepsilon_p + 0.0425\left(1-\varepsilon_p\right)} + \frac{f+1}{\varepsilon_g} - 1} \quad (9)$$

$$f = 1.058 \cdot \left(1 - 0.04 \cdot h_{c,g} + 5 \cdot 10^{-4} \cdot h_{c,g}^2\right) \quad (10)$$

$$h_{c,g} = 5.7 + 3.8 \cdot w \quad (11)$$

It is necessary to underline that Eq. (9) and Eq. (10) only hold for single-glazed collectors. Now, if looking at Eq. (2), whose terms can be specified according to Eq.(3) to Eq. (11), this still contains two unknown variables, namely the plate temperature T_p and the fluid outlet temperature T_{out}. In fact, as concerns the other relevant temperature, i.e. the inlet fluid temperature T_{in}, a constant value will be imposed.

Thus, we need to state one more equation in order to fully describe the thermal performance of the absorber plate. To this aim, it might be useful to treat the element sketched in Fig. 4 as an element of a heat exchanger [2]: this allows to write Eq. (12), where UA_c is the inverse ratio of the overall thermal resistance between the plate surface and the fluid core, as described in Eq. (13).

$$\dot{m}_w \cdot c_{p,w} \cdot \left(T_{out} - T_{in}\right) = -UA_c \cdot \frac{\left(T_{out} - T_{in}\right)}{\ln\left(\frac{T_{out} - T_p}{T_{in} - T_p}\right)} \quad (12)$$

$$UA_c = \left[\frac{1}{h_{c,c} \cdot 4a \cdot 2L} + \frac{\delta_c}{\lambda_c \cdot a \cdot 2L}\right]^{-1} \quad (13)$$

Finally, the internal convective coefficient $h_{c,c}$ can be determined through well-established relationships for forced convection, as a function of both the flow regime and the thermophysical properties of water.

3. ENERGY ANALYSIS: RESULTS

The set of equations presented in the previous section allows, at each time step, the calculation of the following parameters:

- plate temperature, T_p;
- outlet fluid temperature, T_{out};
- useful thermal power, Q_w.

This mathematical model has been applied to the prototype of PV/T collector in order to assess its potential performance in terms of annual thermal and electric energy production. The calculation has been performed on a hourly basis, by using a representative day for each month. Weather data refer to the city of Catania (Italy, latitude = 37°30'), and correspond to those available on the database of the software tool EnergyPlus. In particular, the values of the solar irradiance I_{sol} refer to a surface due south and with a tilt angle 20° on the horizontal plane, that is to say the real configuration of the prototype.

Table 1 reports the constant values of the main geometrical and thermophysical parameters used for the calculation. The water mass flow rate corresponds to 80 $kg \cdot h^{-1} \cdot m^{-2}$, which belongs to the typical range adopted in the design of flat plate solar collectors (40-120 $kg \cdot h^{-1} \cdot m^{-2}$); this value implies a velocity $w = 0.16$ $m \cdot s^{-1}$ for the water flowing inside the channels. On the other hand, the radiation properties of the glazing and the plate ($\tau\alpha$, τ_v) were considered time-dependent, and calculated as a function of the angle of incidence of the solar radiation on the collector surface, according to the formulation available in [3].

Tab. 1 – Main calculation parameters

a = 0.01	[m]	$\lambda_p = \lambda_c = 23$	[W m^{-1} K^{-1}]
W = 0.079	[m]	$\varepsilon_p = 0.9$	[-]
L = 2.966	[m]	$\varepsilon_g = 0.88$	[-]
$c_{p,p} = 502$	[J kg^{-1} K^{-1}]	$\beta = 0.0047$	[$°C^{-1}$]
$\delta_p = 0.6 \cdot 10^{-3}$	[m]	$\eta_{stc} = 0.157$	[-]
$\delta_c = 1 \cdot 10^{-3}$	[m]	$c_{p,w} = 4200$	[J kg^{-1} K^{-1}]
$M_p = 3.9$	[kg]	$\dot{m}_w = 0.082$	[kg s^{-1}]
w = 2	[m s^{-1}]	$T_{in} = 20$	[°C]

Finally, starting from the results of the mathematical model described so far, it is possible to evaluate the overall electric power and thermal power made available by the prototype shown in Fig. 2:

$$P_{el} = \eta_{PV} \cdot I_{sol} \cdot A_{PV} \quad (14)$$

$$\dot{Q}_t = \dot{Q}_w \cdot \frac{A_{tot}}{\left(2L \cdot W\right)} \quad (15)$$

The hourly profiles of the main results in July are reported in Fig. 5 and Fig. 6. One can observe that the water outlet temperature hardly exceeds 26°C, whereas the cell temperature does not overtake 28°C, even when the solar irradiance and the outdoor air temperature are at their height (Fig. 5). This is a consequence of the assumption of T_{in} = 20°C as a constant for the water inlet temperature; in any case, such a result seems to be extremely positive for the PV cells, whose efficiency can benefit a lot from a temperature far lower than that usually occurring in common PV modules.

The electricity production of the PV/T collector reaches 340 W at 12:00 am, but it keeps always lower than the corresponding rate of heat recovery, the latter having a peak value of 2000 W (Fig. 6). For a deeper understanding of these results, it is worth recalling that the electric harvesting of PV cells refers to the packing fraction PF = A_{PV}/A_{tot} = 0.716 of the collector surface, whereas heat recovery pertains to the entire collector surface A_{tot}.

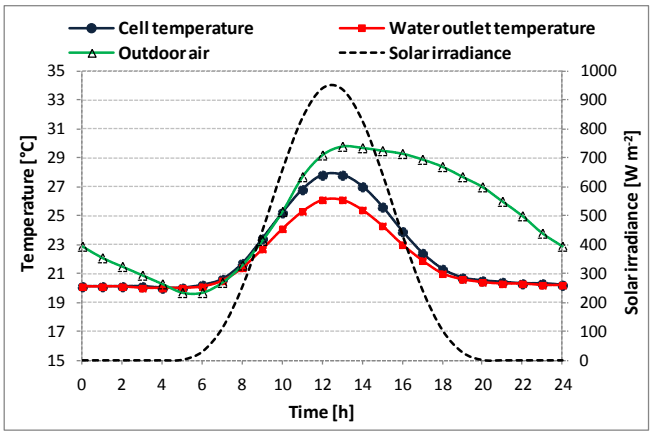

Fig. 5 – Main data for evaluating the energy performance of the PV/T collector (July)

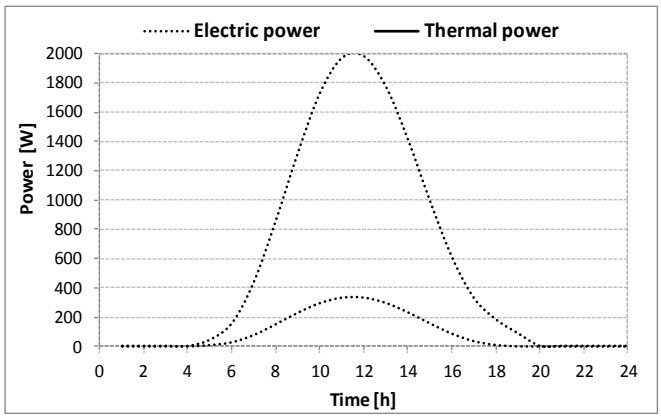

Fig. 6 – Electric and thermal energy produced by the PV/T collector (July)

Furthermore, Fig. 7 reports the hourly values of both the thermal efficiency η_t and the electric efficiency η_{el} of the PV/T collector, plotted against the ratio $x = (T_p - T_a)/I_{sol}$. The points only refer to May, June and July, but allow drawing with a good precision the efficiency curves of the collector. The figure also shows the *total efficiency* η curve, corresponding to the ratio of the overall energy production (electric + thermal) to the available solar radiation:

$$\eta = \frac{\dot{Q}_t + P_{el}}{I_{sol} \cdot A_{tot}} = \eta_t + PF \cdot \eta_{el} \qquad (16)$$

The equation of the thermal efficiency reported in Fig. 7 suggests that the thermal performance of the PV/T collector is not as good as for traditional flat plate solar collectors: indeed, these show an average peak efficiency $\eta_0 = 0.7 \div 0.75$ (whereas in this case: $\eta_0 = 0.62$), and the slope of the efficiency curve is usually around $4 \div 5$ W·m^{-2}·K^{-1} (when it 6.62 W·m^{-2}·K^{-1} for this PV/T collector). This outcome can be justified by the presence of the PV cells, that convert part of the solar radiation into electric energy, and by considering that the heat losses to the environment are relevant due to high thermal emissivity (ε_p = 0.9).

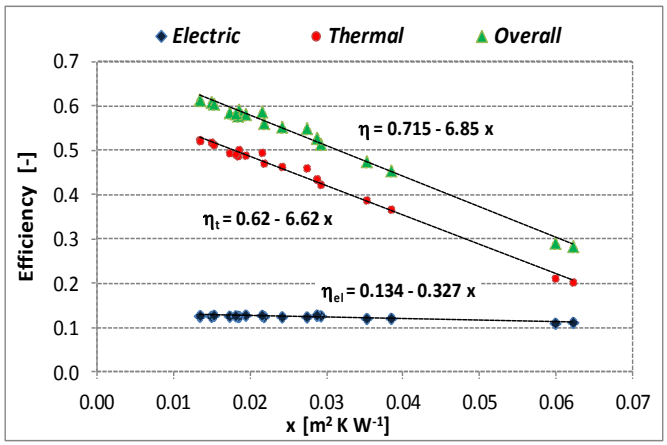

Fig. 7 – Efficiency curves for the prototype of PV/T collector

Finally, the evaluation of the monthly average performance of the PV/T collector, in terms of energy production and efficiency, can be done by Eqs. (17).

$$\bar{\eta}_{el} = \frac{\int_{day} P_{el}(t) \cdot dt}{\int_{day} I_{sol}(t) \cdot A_{PV} \cdot dt} \qquad \bar{\eta}_t = \frac{\int_{day} \dot{Q}_t(t) \cdot dt}{\int_{day} I_{sol}(t) \cdot A_{tot} \cdot dt} \qquad (17)$$

It is also useful to define a further parameter, called *primary energy efficiency*, as in Eq. (18): it accounts for the primary energy consumption, per unit solar radiation, avoided thanks to the use of a PV/T collector:

$$\bar{\eta}_{PE} = \frac{\frac{1}{\eta_{net}} \cdot \int_{day} P_{el}(t) \cdot dt + \frac{1}{\eta_{hg}} \cdot \int_{day} \dot{Q}_t(t) \cdot dt}{\int_{day} I_{sol}(t) \cdot A_{tot} \cdot dt} \qquad (18)$$

In this formula η_{hg} and η_{net} represent the reference values respectively for a common gas boiler (as a conventional technology to produce heat) and for the electric system on a nationwide basis. The adopted values are as follows: η_{net} = 0.46 and η_{hg} = 0.9.

The results of this calculation are shown in Fig. 8 and Fig. 9. Here, one can learn that the daily energy production of the PV/T collector experiences a considerable swing throughout the year. In particular, the electricity production lays in the range 0.6 ÷ 2.3 kWh/day from December to July (Fig. 8). Nevertheless, the electric efficiency keeps quite constant, as it oscillates between 13.3% and 13.5% (Fig. 9): the lowest values occur in summer, when the overheating of the PV cells is more pronounced.

On the other hand, the thermal performance is highly penalized in winter, when the average thermal efficiency is between 30% and 40%, while this exceeds 50% within the period May - October. The primary energy efficiency shows a similar trend, with a peak value around 85% in July and August.

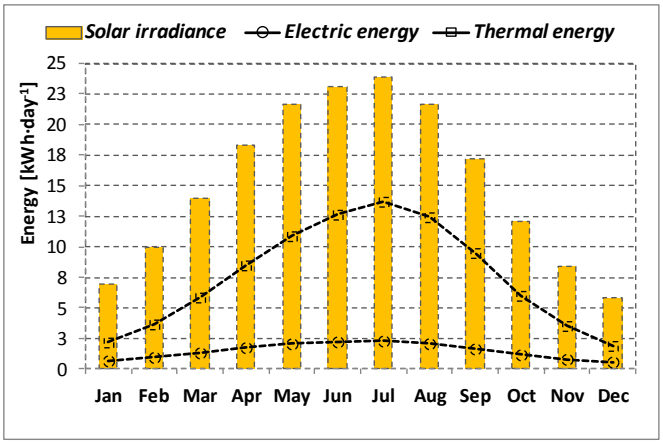

Fig. 8 – Mean monthly values of the energy harvested by the PV/T collector

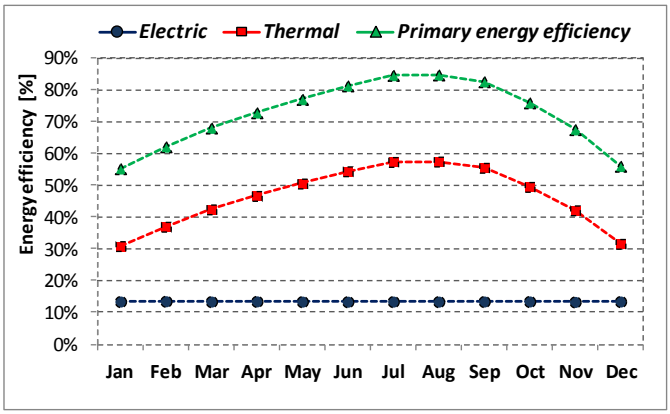

Fig. 9 – Mean monthly values for the PV/T energy efficiency

4. EXERGY ANALYSIS

4.1 *Definition of the methodology*

The analysis presented in the previous section, concerning the energy performance of the prototype of PV/T collector, is basically founded on the First Law of Thermodynamics. However, according to this approach the thermal and electric energy harvested by the system can be evaluated and compared just under a merely *metric* criterion, with no reference to their actual thermodynamic quality. On the contrary, only the Second Law of Thermodynamics would allow a proper evaluation of the quality of each energy flow.

To this aim the concept of *exergy* or *available energy* should be used: this measures the maximum useful work that can be obtained during a process that brings the system to a complete equilibrium (thermal, chemical, mechanical) with the environment. Now, while electric energy is *pure exergy*, thermal energy has an *exergy content* that depends on the temperature at which heat is made available.

In the recent scientific literature, some works have already tackled the exergy analysis of both water-cooled and air-cooled PV/T collectors [5-12], with a certain discrepancy among the Authors.

In this paper, the exergy content of a mass flow, can be calculated by the fundamental equation [13]:

$$E_Q = \dot{m}_w \cdot \left[h_{out} - h_{in} - T_0 \cdot (s_{out} - s_{in}) \right] \tag{19}$$

Now let us introduce the Mean Thermodynamic Temperature $T_m = (h_{out} - h_{in}) / (s_{out} - s_{in})$ which, for a liquid (or ideal gas) flow experiencing a heating process from the inlet T_{in} to the outlet T_{out} temperature, can be expressed as:

$$T_m = \frac{T_{out} - T_{in}}{\ln(T_{out} / T_{in})} \tag{20}$$

As to the definition of T_0 for the reference state (*dead state*), some Authors adopt the time-varying profile of the outdoor temperature [9, 12]. However, Pons stated that it is not correct to consider a variable T_0, as this introduces a series of thermodynamic contradictions [14]. Thus, a constant T_0 is assumed in this paper; in particular, its value corresponds to the minimum outdoor temperature for any given month.

In this context it is suitable now to introduce the energy efficiency of the PV/T panel considered as a thermal collector (Eq. 21) which, on the basis of the curves shown in Fig. 7, can be assessed also as a function of T_p, T_a, and I_{sol} as follows :

$$\eta_t = \frac{\dot{m}_w \cdot c_{p,w} \cdot (T_{out} - T_{in})}{I_{sol} \cdot A_{tot}} = 0.62 - 6.62 \cdot \frac{T_p - T_a}{I_{sol}} \tag{21}$$

Collecting equations (20) and (21), Eq. (19) can be re-written as:

$$E_Q = \dot{m}_w c_{p,w} (T_{out} - T_{in}) \cdot \left(1 - \frac{T_0}{T_m}\right) = \eta_t I_{sol} A_{tot} \left(1 - \frac{T_0}{T_m}\right) \tag{22}$$

As to the exergy of the electric power, it is to remind that it is pure exergy. Thus:

$$E_{el} = P_{el} = \eta_{PV} \cdot I_{sol} \cdot PF \cdot A_{tot} \tag{23}$$

Finally, one needs to assess the exergy content of the solar radiation incident on the collector surface. In this paper, the authors adopt the following formula proposed by Petela [15], where T_{sol} = 5760 K is the apparent solar temperature.

$$e_{sol} = I_{sol} \cdot \underbrace{\left[1 - \frac{4}{3} \cdot \frac{T_0}{T_{sol}} + \frac{1}{3} \cdot \left(\frac{T_0}{T_{sol}}\right)^4\right]}_{C_{sol}} \approx 0.935 \cdot I_{sol} \tag{24}$$

Slightly different approaches in the literature are proposed by Pons [16] and Jeter [17]. On the basis of the previously stated model, it is possible to define the average exergy efficiency of both the electricity production (ξ_{el}) and the thermal exergy recovery (ξ_t) for each month. To this aim Eq. (25) will be used.

$$\overline{\xi}_{el} = \frac{\int_{day} E_{el}(t) \cdot dt}{\int_{day} e_{sol}(t) \cdot A_{PV} \cdot dt} \qquad \overline{\xi}_{t} = \frac{\int_{day} E_{Q}(t) \cdot dt}{\int_{day} e_{sol}(t) \cdot A_{tot} \cdot dt} \tag{25}$$

For the *overall exergy efficiency* of the PV/T collector, that is the ratio of the overall exergy production to the exergy of the solar radiation available on the collector plane, Eq. (26) can be reasonably stated:

$$\overline{\xi} = \frac{\int_{day} E_{el}(t) \cdot dt + \int_{day} E_{Q}(t) \cdot dt}{\int_{day} e_{sol}(t) \cdot A_{tot} \cdot dt} = \overline{\xi}_{el} \cdot PF + \overline{\xi}_{t} \tag{26}$$

4.2 *Results*

The results of this analysis are shown in Fig. 11. They seem quite deceiving if compared with those of the energy analysis of Fig. 9. In fact, the average thermal exergy efficiency only ranges between 0.5% and 2.5%, with the lowest values occurring in the hottest months, when the energy efficiency is at its height (around 60%, see Fig. 9).

This happens because, despite the PV/T collector is able to convert a relatively high portion of the available solar energy into useful heat, such heat is made available at a temperature that is very close to the ambient temperature (25-30°C), which makes the heat scarcely useful on a technical basis.

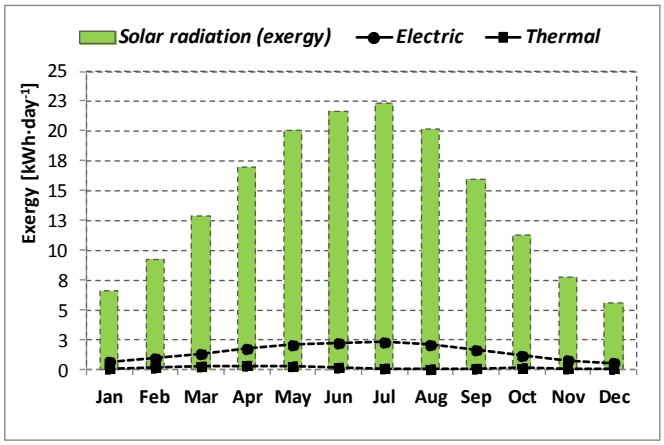

Fig. 10 – Mean monthly values for the exergy production from the PV/T collector

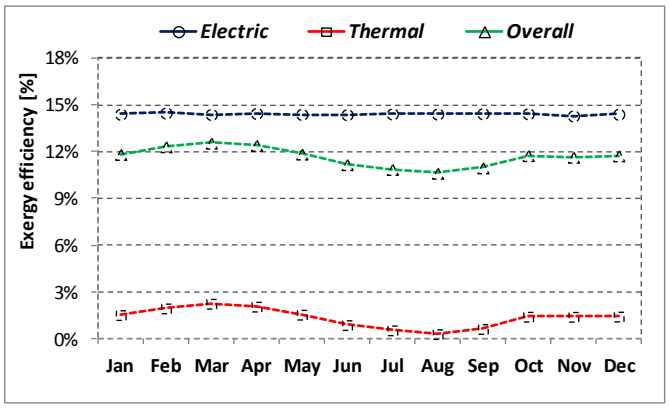

Fig. 11 – Mean monthly values for the PV/T exergy efficiency

On the other hand, the Second Law approach enhances the value of the electricity production, as this can be entirely converted into useful work, whatever the temperature of the system. Hence, the production of *electric exergy* from the PV/T collector is constantly higher than the corresponding *thermal exergy* production (see Fig. 10).

One can also observe that the electric *exergy efficiency* overtakes the electric *energy efficiency*: indeed, while η_{el} oscillates between 13.3% and 13.5% (Fig. 9), ξ_{el} gets close to 14.5% (Fig. 11). This difference arises because, for a given energy output, the energy and the exergy content of the solar radiation is not the same, due to the Petela conversion factor $C_{sol} \approx 0.935$ (Eq. 24).

5. THERMODYNAMIC OPTIMIZATION

The investigations based on the First Law of Thermodynamics seem to suggest low temperature operation for the PV/T panel in order to maximize its overall energy efficiency (Fig. 7). Actually, this outcome might be misleading: even a high amount of heat is almost useless if available close to the environmental temperature.

For the same reason, the flattering results shown in Fig. 9 should also be critically reconsidered in relation to the Second Law of Thermodynamics. To this aim, it is suitable to introduce the overall exergy efficiency ξ:

$$\xi = \frac{E_{el} + E_Q}{I_{sol} \cdot A_{tot} \cdot C_{sol}} \tag{27}$$

which, on the basis of previous equations, can be re-written in the following form:

$$\xi = \frac{\eta_{PV}}{C_{sol}} \cdot PF + \frac{\eta_t}{C_{sol}} \cdot \left[1 - \frac{T_0}{T_m}\right] \tag{28}$$

Now, it turns out that, in the right-hand side of Eq. (28), the first term is decreasing, while the second one is increasing with the inlet temperature T_{in}. As a result, the curve presents a maximum, as shown in Fig. 12.

The plot refers to a mass flow rate $\dot{m}_w$ = 80 kg·h^{-1}·m^{-2} and to three different combinations of I_{sol} and T_a (which tackle typical operating conditions). The curves show that, for each operating condition, it is possible to determine an optimal fluid inlet temperature $(T_{in})_{opt}$, such as to maximize the overall exergy efficiency. Moreover, such an optimal temperature is also technically feasible, as it belongs to the range commonly occurring in solar thermal systems; i.e. from 25°C (when I_{sol} = 400 W·m^{-2} and T_a = 15°C) to 45°C (when I_{sol} = 900 W·m^{-2} and T_a = 35°C).

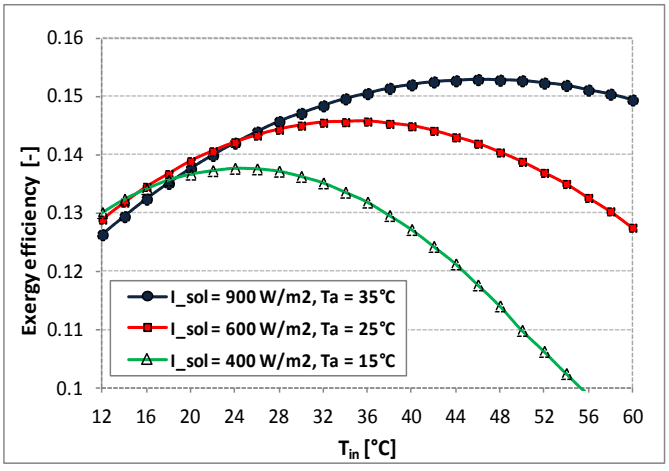

Fig. 12 – Exergy efficiency of the PV/T system as a function of the water inlet temperature

The exergy efficiency can then be considered a multivariable function, such as :

$$\xi = f(T_{in}, \dot{m}_w, I_{sol}, T_a)$$

which suggests a way to achieve the best PV/T performance from the Second Law point of view. To this aim, one can conceive a solar loop with a three-way control valve installed on the water supply line, intended to feed the PV/T collector

with water at the optimal supply temperature $(T_{in})_{opt}$, which in turn can be determined, for each time step, as a function of the measured values of $\dot{m}_w$, I_{sol} and T_a. Such a control system would allow the system to work constantly at the highest overall exergy efficiency.

6. CONCLUSIONS

This paper concerns a prototype of water-cooled glazed PV/T collector, developed in the framework of an Italian research project. The study aims at evaluating the energy performance of the collector, in the light of both the First and the Second Law of Thermodynamics; the evaluation is based on a mathematical model for the dynamic simulation of the system.

The results suggest that the outcomes of the First Law are misleading, as the thermal energy produced by the system, even in high quantities, is almost useless when available at low temperatures. On the contrary, the adoption of the Second Law of Thermodynamics, based on the concept of exergy, can properly evaluate the quality of the thermal energy, associated with its temperature level. In this case, it is possible to identify – for each operating condition – an optimal value for the water inlet temperature, that allows maximizing the overall exergy efficiency. Such outcomes can be used to define a control logic that might be implemented in a control system for the thermodynamic optimization of the PV/T system.

All that will be the subject of a forthcoming paper, which will investigate how much exergy (and energy) can be collected by the PV/T under these operating conditions, and what could be the economic value of heat, according to its temperature level or exergy content (thermo-economic analysis).

NOMENCLATURE

a	external side of the channel	m
A	surface area	m^2
c_p	specific heat	J kg^{-1} K^{-1}
C_{sol}	corrective coefficient	-
e	exergy per unit surface	W m^{-2}
E	exergy	W
F	fin efficiency	-
h	specific enthalpy	J kg^{-1}
h_c	convective coefficient	W m^{-2} K^{-1}
I	solar irradiance	W m^{-2}
L	length	m
$\dot{m}$	mass flow rate	kg s^{-1}
M	mass	kg
P_{el}	electric power	W
PF	packing factor	-
$\dot{Q}$	thermal power	W
s	specific entropy	J kg^{-1}
t	time	s
T	temperature	K
U	overall heat transfer coefficient	W m^{-2} K^{-1}
w	velocity	m s^{-1}
W	width of the absorber plate	m

Greek symbols

α	absorptivity	-
β	temperature coefficient	$°C^{-1}$
δ	thickness	m
ε	thermal emissivity	-
η	energy efficiency	-
λ	thermal conductivity	W m^{-1} K^{-1}
ξ	exergy efficiency	-
σ	Stefan-Boltzmann constant	W m^{-2} K^{-4}
τ	transmittance	-
ψ	latitude	°

Subscripts

a	outdoor air
c	channel
el	electric
g	glass
hg	heat generator
in	inlet
l	losses
out	outlet
p	absorber plate
PE	primary energy
PV	photovoltaic panel/cells
net	electricity distribution network
STC	standard test conditions
t	thermal
tot	total
w	water
0	reference, dead state

REFERENCES

1. M. Cucumo, D. Cucumo, A. De Rosa, V. Ferraro, D. Kaliakatsos, V. Marinelli, Analisi teorica di un collettore solare cogenerativo PV/T a liquido, Atti Congresso Nazionale ATI, 2009.
2. N. Aste and F. Groppi, Impianti solari termici – Manuale per ingegneri, architetti, installatori, Editoriale Delfino, Milano, 2007.
3. W.A. Beckman and A. Duffie, Solar Engineering of thermal processes, John Wiley & Sons, 1980.
4. H.A. Zondag, D.W. de Vries, W.G.J. van Helden, R.J.C. van Zolingen, A.A van Steenhoven, The thermal and electrical yield of a PV-thermal collector, *Solar Energy*, vol. 72 (2), pp. 113-128, 2002.
5. T. Fujisawa and T. Tani, Annual exergy evaluation on photovoltaic-thermal hybrid collector, *Solar Energy Materials and Solar Cells*, vol. 47, pp. 135-148, 1997.
6. J.S. Coventry and K. Lovegrove, Development of an approach to compare the 'value' of electrical and thermal output from a domestic PV/thermal system, *Solar Energy*, vol. 75, pp. 63-72, 2003.
7. A.S. Joshi and A. Tiwari, Energy and exergy efficiencies of a hybrid photovoltaic-thermal (PV/T) air collector, *Renewable Energy*, Vol. 32, pp. 2223-2241, 2007.
8. A.D. Sahin and M. Rosen, Thermodynamic analysis of solar photovoltaic cell systems, *Solar Energy Materials and Solar Cells*, vol. 91, pp. 153-159, 2007.
9. T.T. Chow, G. Pei, K.F. Fong, Z. Lin, A.L.S. Chan, J. Ji, Energy and exergy analysis of photovoltaic-thermal collector with and without glass cover, *Applied Energy*, Vol. 86, pp. 310-316, 2009.

10. R. Saidur, G. BoroumandJazi, S. Mekhlif, M. Jameel, Exergy analysis of solar energy applications, *Renewable and Sustainable Energy Reviews*, Vol. 16, pp. 350-356, 2012.
11. S. Agrawal and G.N. Tiwari, Energy and exergy analysis of hybrid micro-channel photovoltaic thermal module, *Solar Energy*, Vol. 85, p. 356-370, 2011.
12. S. Agrawal and G.N. Tiwari, Overall energy, exergy and carbon credit analysis by different types of hybrid photovoltaic thermal air collectors, *Energy Conversion and Management*, Vol. 65, pp. 628-636, 2013.
13. A. Bejan and M.J. Moran, Thermal Design and Optimization, John Wiley & Sons, 1996.
14. M. Pons, On the reference state for exergy when ambient temperature fluctuates, *International Journal of Thermodynamics*, vol. 12 (3), pp. 113-121, 2009.
15. R. Petela, Exergy of heat radiation, *ASME Transaction Journal of Heat Transfer*, vol. 2, pp. 187-192, 1964.
16. M. Pons, Exergy analysis of solar collectors, from incident radiation to dissipation, *Renewable Energy*, vol. 47, pp. 194-202, 2012.
17. S.M. Jeter, Maximum conversion efficiency for the utilization of direct solar radiation, *Solar Energy*, vol. 26 (3), pp. 231-236, 1981.

ACKNOWLEDGEMENTS

This research has been developed in the framework of the industrial research project on "New Photovoltaic Technologies for Intelligent Systems Integrated in Buildings" (PON 01_01725), financed by the Italian National Program on Research and Competitiveness 2007-2013.